Supporting information for

Synergism of CoO-Ni(OH)$_2$ nanosheets and MOF-derived CNTs array for methanol electrolysis

Kuan Deng,[a] *Peng Liu,*[a] *Xuesong Liu,*[a] *Hongjiao Li,*[a] *Wen Tian,*[a] *Junyi Ji,*[a, b,]*

[a] School of Chemical Engineering, Sichuan University, Chengdu 610065, P. R. China

[b] State Key Laboratory of Polymer Materials Engineering, Sichuan University, Chengdu 610065, P. R. China

* Corresponding author.

Junyi Ji, E-mail: junyiji@scu.edu.cn

SUPPLEMENTARY EXPERIMENTAL SECTION

EXPERIMENTAL SECTION

All chemicals and regents were analytical grade and were used without further purification.

Synthesis of ZnO nanorod arrays on carbon cloth

ZnO nanorod arrays were grown on carbon cloth (CC) by a facile hydrothermal process. The carbon cloth was ultrasonic cleaned by ethanol and DI water, and soaked in $KMnO_4$ solution to improve its hydrophilicity. 0.3 g zinc acetate dihydrate ($Zn(Ac)_2 \cdot 2H_2O$) was dissolved in 30 mL anhydrous ethanol to form seed solution. The cleaned CC was immersed in the seed solution at 40 °C for 1 h, and then annealed at 350 °C for 2 h. The pretreated CC was immersed in solution containing 0.5355 g zinc nitrate hexahydrate ($Zn(NO_3)_2 \cdot 6H_2O$), 0.252 g Hexamethylenetetramine (HMT), 1 mL ammonia (25-28%), 30 mL H_2O and heated at 90 °C for 24 h. Later, the ZnO/CC was rinsed by DI water and dried at 60 °C overnight.

Synthesis of carbon nanotubes (CNTs) arrays on carbon cloth

In a typical experiment, 8.2 g 2-methylimidazole was dissolved in a 50 mL mixed solution of DI water and methanol (1:1 of V/V). A piece of ZnO/CC was soaked into the above solution at 30 °C for 12 h to prepare the ZnO@ZIF-8/CC, followed by annealed under 600 °C for 1 h and increased to 800 °C for 0.5 h in Ar/H_2 (95/5) atmosphere to prepare the CNTs on CC.

Synthesis of CNTs@CoO-Ni(OH)$_2$ on carbon cloth

The nanosheets of CoO-$Ni(OH)_2$ were grown onto the CNTs *via* a two-step

electrodeposition method. Here, the as-synthesized CNTs was applied as the working electrode, the Ag/AgCl and a Pt plate as the reference electrode and counter electrode, respectively. First, the $Ni(OH)_2$ nanosheets were prepared on CNTs by galvanostatic electrolysis in 70 mL solution of 50 mM $Ni(NO_3)_2$ at -5 mA cm^{-2} for 200 s. Then, the CoO-$Ni(OH)_2$ were synthesized by the second electrodeposition in the solution of 5 mM $CoSO_4$ and 5 mM sodium citrate at -1 mA cm^{-2} for 100 s (CNTs@CoO-$Ni(OH)_2$-100), 200 s (CNTs@CoO-$Ni(OH)_2$-200), 300 s (CNTs@CoO-$Ni(OH)_2$-300), 400 s (CNTs@CoO-$Ni(OH)_2$-400). For the comparative study, the CoO-$Ni(OH)_2$/CC and CNTs@CoO were also synthesized with the similar methods described above.

Material characterization

Transmission electron microscopy (TEM, JEM-F200, JEOL) and Field Emission Scanning Electron Microscopy (SEM, JSM-7610F, JEOL) along with an energy dispersive X-ray spectrometry (EDS) were used to understand the structure of the composites. The X-ray diffractometer (XRD, Cu Kα radiation, DX2700, Dandong Haoyuan) was used to identify crystal structures. The elemental valence states were tested by X-ray photoelectron spectroscopy (XPS, PHI 5000 Versa spectrometer). The Raman was performed using a DXR spectrometer (Thermal Scientific, 455 nm). The composition of electrolyte at the anode was determined by nuclear magnetic resonance (NMR, JNM-ECZ400S/L1, JEOL Ltd., Japan).

Electrochemical measurements

The electrochemical measurements were conducted using a standard three-electrode system configuration on CHI 760E electrochemical workstation (CH

Instruments, Ins. Shanghai, China) and Autolab electrochemical workstation (Metrohm Autolab M204, the Netherlands). A carbon rod electrode and Hg/HgO electrode used as the counter electrode and reference electrode, respectively. 1 M KOH or 1 M KOH+1 M CH_3OH was used as electrolyte. Linear sweep voltammetry (LSV) measurement was conducted at a scan rate of 5 mV s^{-1}. Presented potentials were normalized to reversible hydrogen electrode (RHE) according to the equation: $E_{RHE} = E_{Hg/HgO} + 0.059 * pH + 0.098$. The LSV measurement results were fitted and calculated to obtain the Tafel slope. The equation formula of the Tafel curves is: $\eta = a + b * log|j|$. η represents the overpotential (RHE), b represents the Tafel slope and j is the current density. Electrochemical impedance spectroscopy (EIS) was measured from 0.01 to 10^5 Hz with an amplitude of 5 mV. Cyclic voltammetry (CV) experiments were conducted in non-Faradic current region with different scanning rates from 10 to 70 mV s^{-1} to determine the double layer capacitances (C_{dl}) values of the catalysts. The stability measurements were carried out using chronoamperometry with *i-t* curves conducted at a constant working potential.

The surface coverage of Ni^{2+}/Ni^{3+} redox species in the catalysts were studied based upon the linear relation between the peak current density values of the Ni^{2+}/Ni^{3+} redox couple and the scan rate using CV measurement. The CVs of the catalyst in 1 M KOH solution at different scan rates from 10 to 100 mV s^{-1} were performed. The anodic and cathodic peak current densities enlarged with increased scan rate. However, due to the limitation of the reaction kinetics, the time for the complete formation of Ni^{2+} was insufficient at higher scan rate. Thus, the peak potentials displayed a hysteresis effect.

It is clear that the peak current densities of the Ni^{2+}/Ni^{3+} redox couple are linearly proportional to the scan rate.

The surface coverage (Γ^*) of Ni^{2+}/Ni^{3+} redox species and the proton diffusion coefficient (D) was calculated by the *Randles-Sevcik* equation as follows:

$$I_p = \left(\frac{n^2F^2}{4RT}\right)A\Gamma^* v$$

Where I_p is the peak current, n is the number of transferred electrons, F is the Faraday constant, R is the general gas constant, T is the temperature, A is the geometrical electrode surface area, v is the potential scan rates.

$$I_p = 2.69\times10^5 n^{3/2} A D^{1/2} C v^{1/2}$$

Where I_p is the peak current, n is the number of transferred electrons, A is the geometrical electrode surface area and C is the initial concentration of redox species that, taking into account a $Ni(OH)_2$ density of 3.97 g cm^{-3}, we estimated at 0.043 mol cm^{-3}.

Production analysis

The electrolyte at the anode for MOR was used for nuclear magnetic resonance (NMR) to determine the products of MeOH oxidation and calculate Faradaic efficiencies. ^{13}C NMR and quantitative ^{1}H NMR spectra were recorded on a JNM-ECZ400S/L1 NMR. During the measurement, 1 mL electrolyte was added into 0.6 mL D_2O, and maleic acid used as an internal standard. The Faradic efficiencies (FE) for the production of formate were calculated using the following equation:

$$FE = \frac{n \times z \times F}{Q} \times 100\%$$

Where n is the yield of formate (mol), z is the number of electron transfer for each product formation (z=4), Q is the quantity of electric charge (C), F is the Faraday constant (96458 C mol^{-1}).

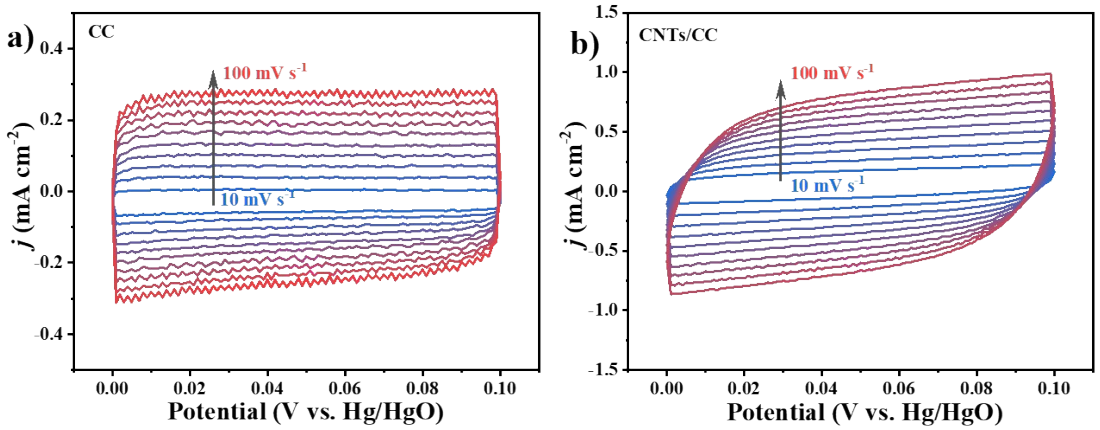

Figure S1 CV curves of the a) CC, and b) CNTs/CC at 10, 20, 30, 40, 50, 60, 70, 80, 90 and 100 mV s^{-1}.

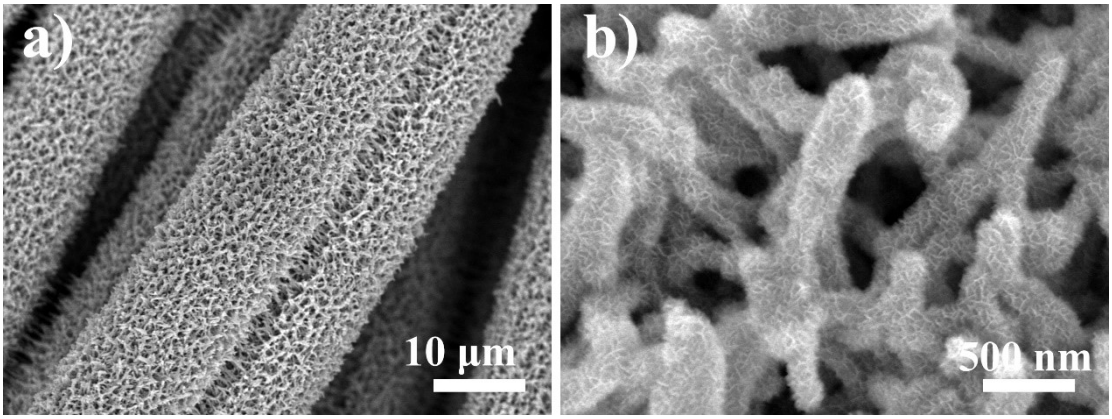

Figure S2 SEM images of the a, b) CNTs@$Ni(OH)_2$/CC composite.

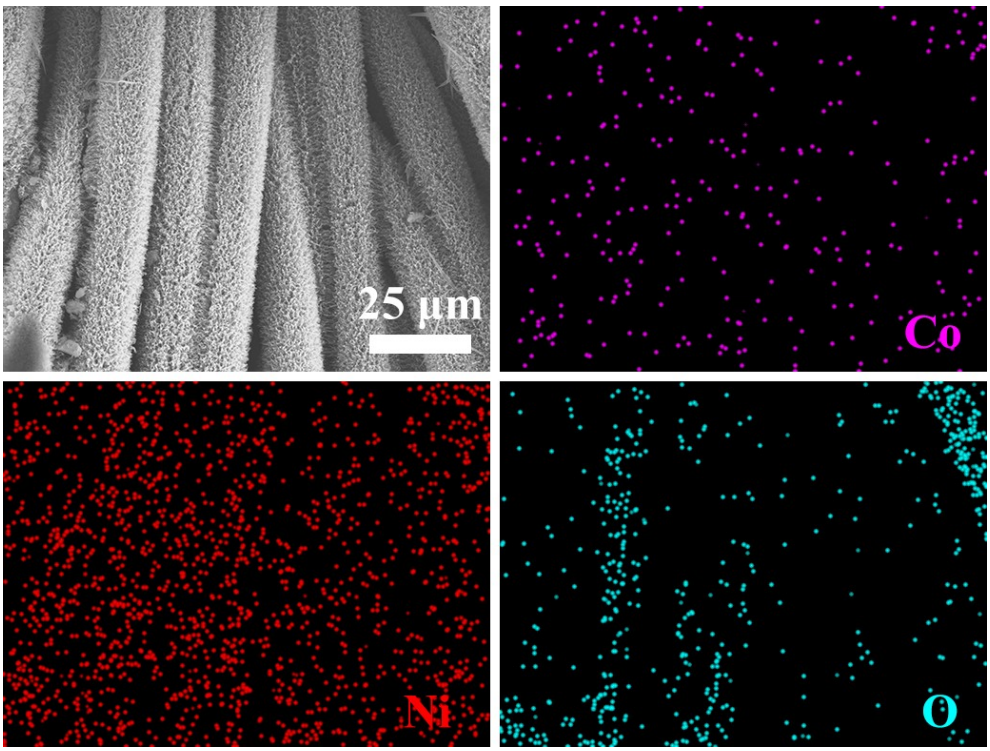

Figure S3 SEM image and corresponding EDS mapping of the CNTs@CoO-$Ni(OH)_2$ composite.

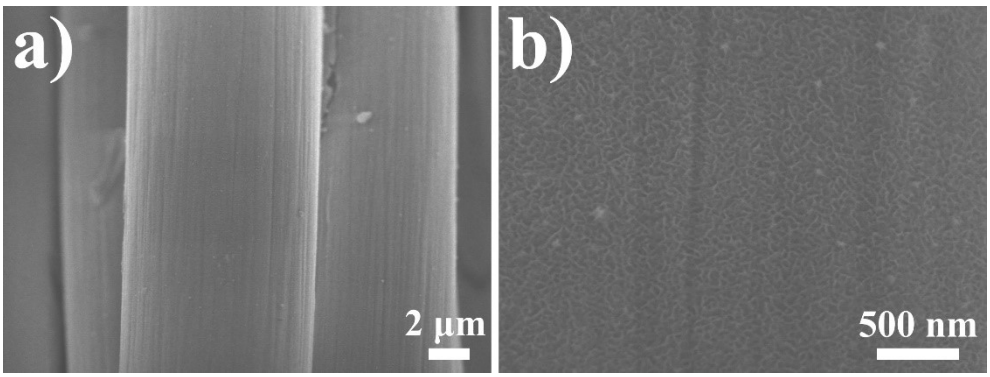

Figure S4 SEM images of the CoO-$Ni(OH)_2$/CC composite.

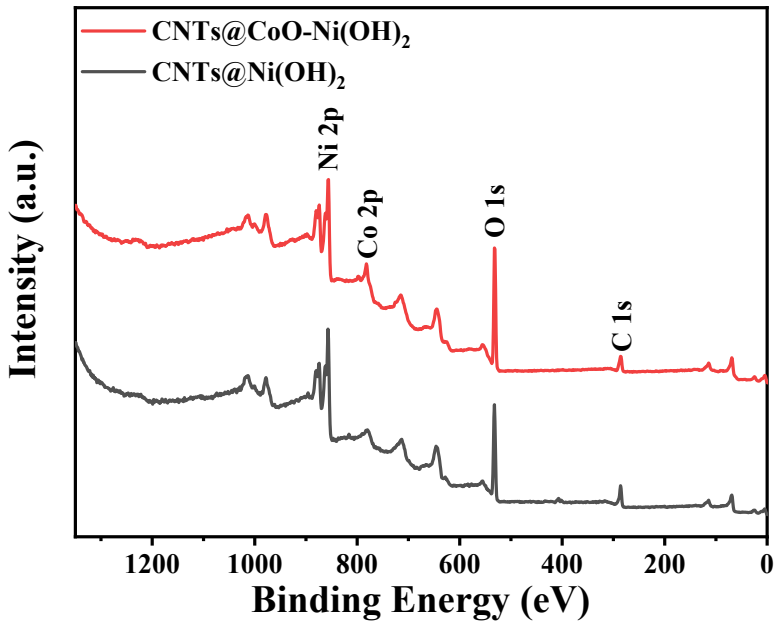

Figure S5 Full XPS survey spectrum of the CNTs@$Ni(OH)_2$ and CNTs@CoO-$Ni(OH)_2$ composites.

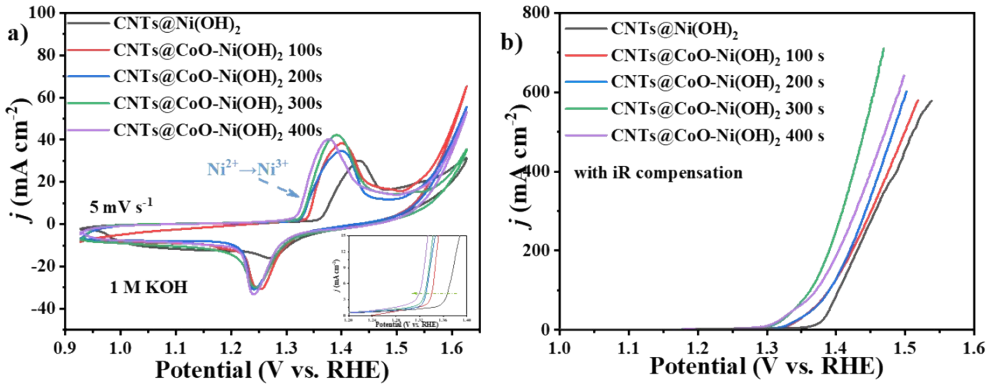

Figure S6 a) CV curves of the CNTs@$Ni(OH)_2$ and CNTs@CoO-$Ni(OH)_2$ x (x=100, 200, 300, 400 s) at 5 mV s^{-1} in 1 M KOH, b) LSV curves of the CNTs@$Ni(OH)_2$ and CNTs@CoO-$Ni(OH)_2$ x (x=100, 200, 300, 400 s) in 1 M KOH with 1 M MeOH.

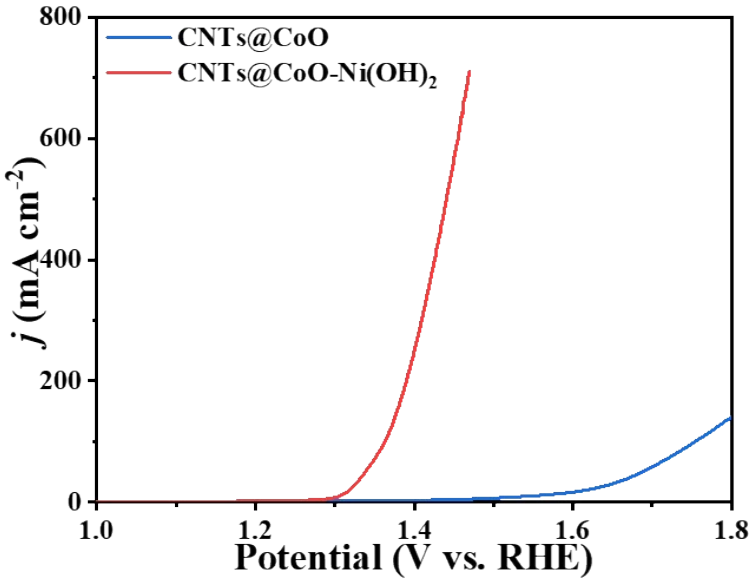

Figure S7 LSV curves of the CNTs@CoO-Ni(OH)$_2$ and CNTs@CoO in 1 M KOH with 1 M MeOH.

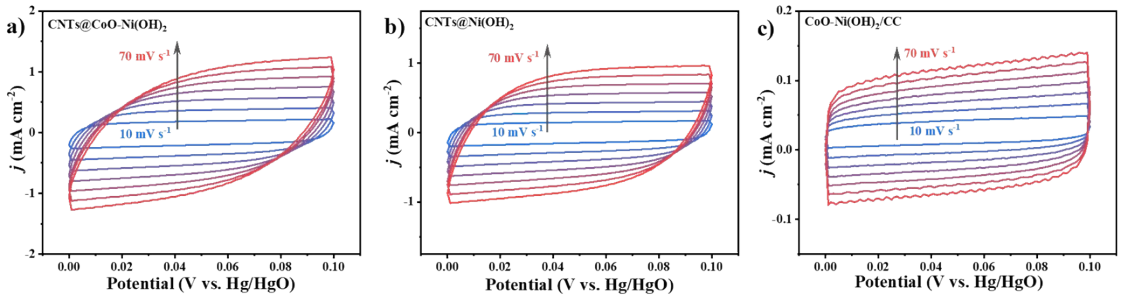

Figure S8 CV curves of the a) CNTs@CoO-Ni(OH)$_2$, b) CNTs@Ni(OH)$_2$, and c) CoO-Ni(OH)$_2$/CC at 10, 20, 30, 40, 50, 60, and 70 mV s^{-1}.

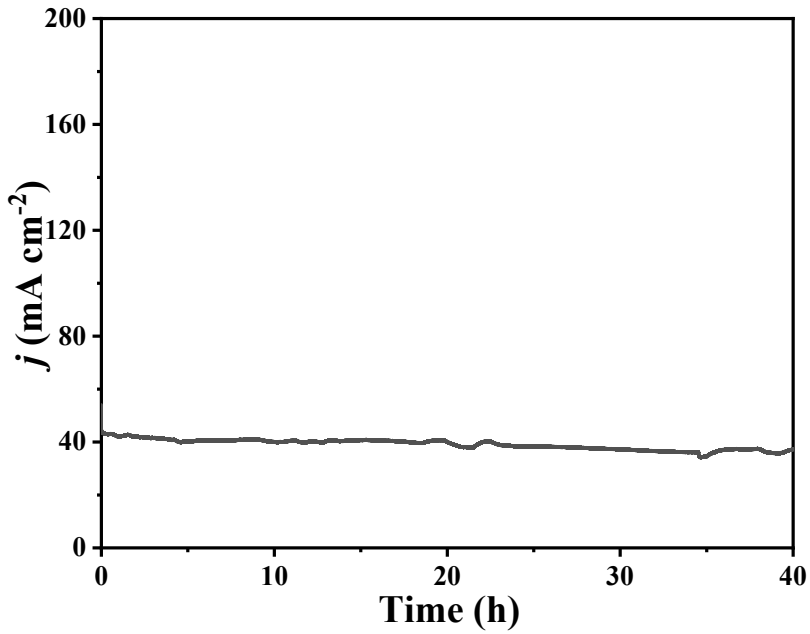

Figure S9 Chronoamperometry curve of the CNTs@CoO-Ni(OH)$_2$ electrode in 1 M KOH with 1 M CH_3OH.

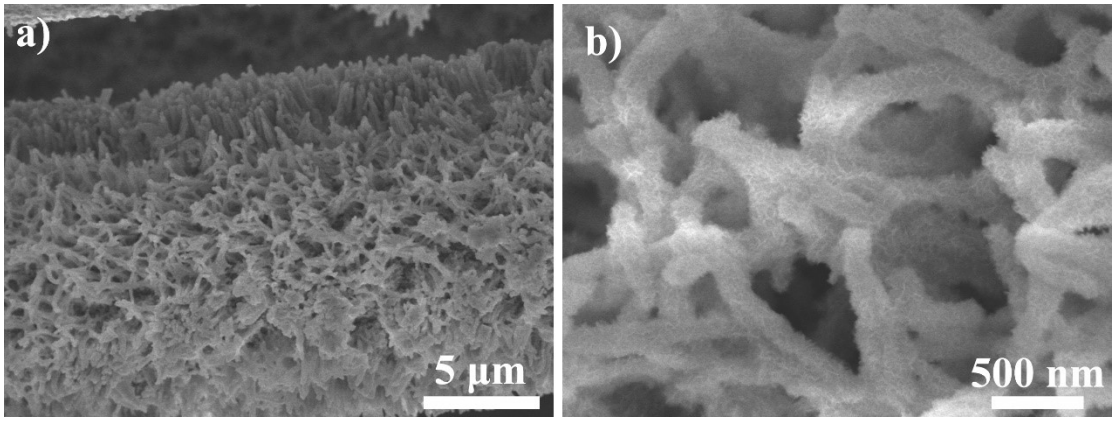

Figure S10 SEM images of the CNTs@CoO-Ni(OH)$_2$ after long-term chronoamperometry test.

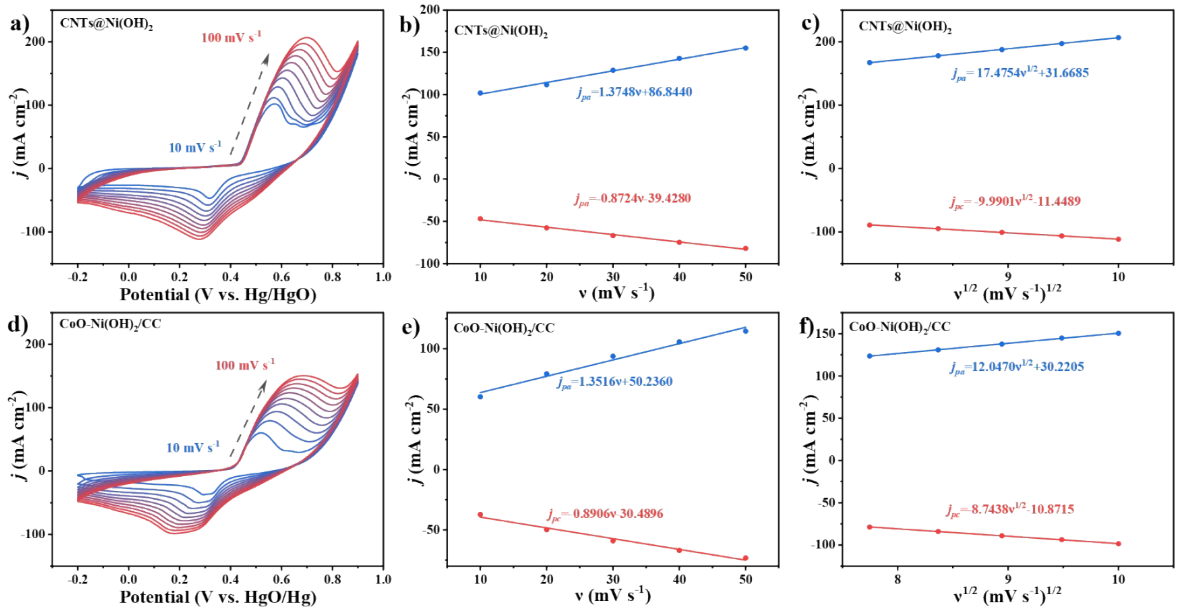

Figure S11 a) CV curves of CNTs@Ni(OH)$_2$ in 1 M KOH at scanning rate from 10 mV s^{-1} to 100 mV s^{-1}. Relationship between anodic and cathodic current densities to b) the scan rates, and c) the square root of the scan rates of CNTs@Ni(OH)$_2$. d) CV curves of CoO-Ni(OH)$_2$/CC in 1 M KOH at scanning rate from 10 mV s^{-1} to 100 mV s^{-1}. Relationship between anodic and cathodic current densities to e) the scan rates, and f) the square root of the scan rates of CoO-Ni(OH)$_2$/CC.

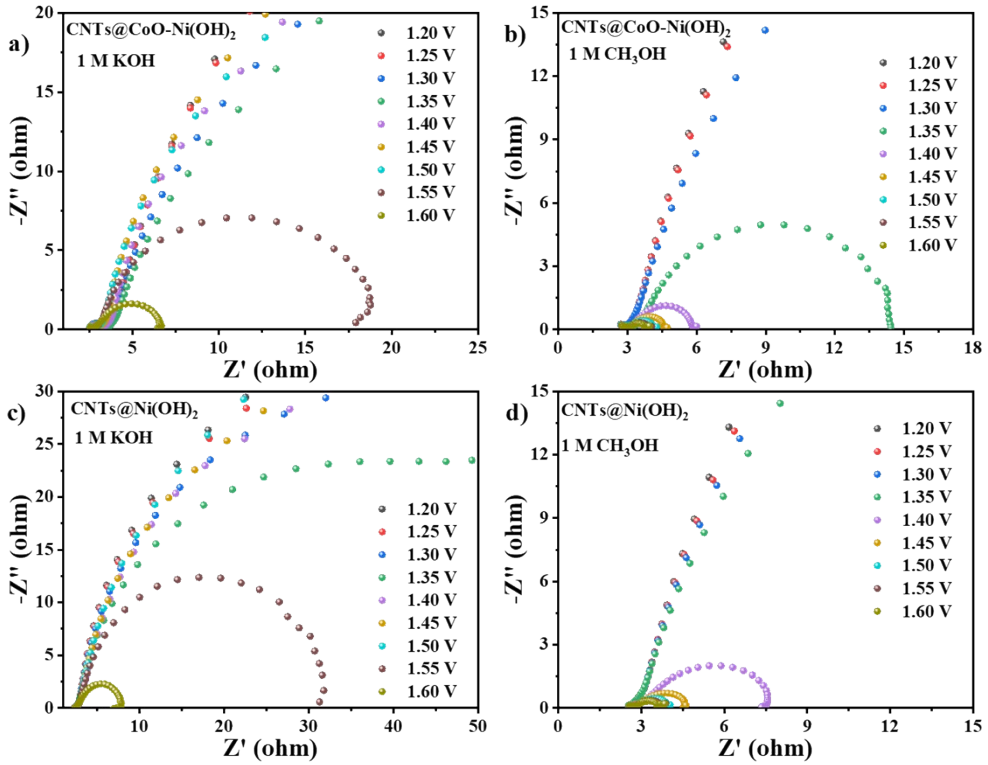

Figure S12 Nyquist plots of CNTs@CoO-Ni(OH)$_2$ in a) 1 M KOH and b) 1 M KOH+1 M CH_3OH. Nyquist plots of CNTs@Ni(OH)$_2$ in c) 1 M KOH and d) 1 M KOH+1 M CH_3OH

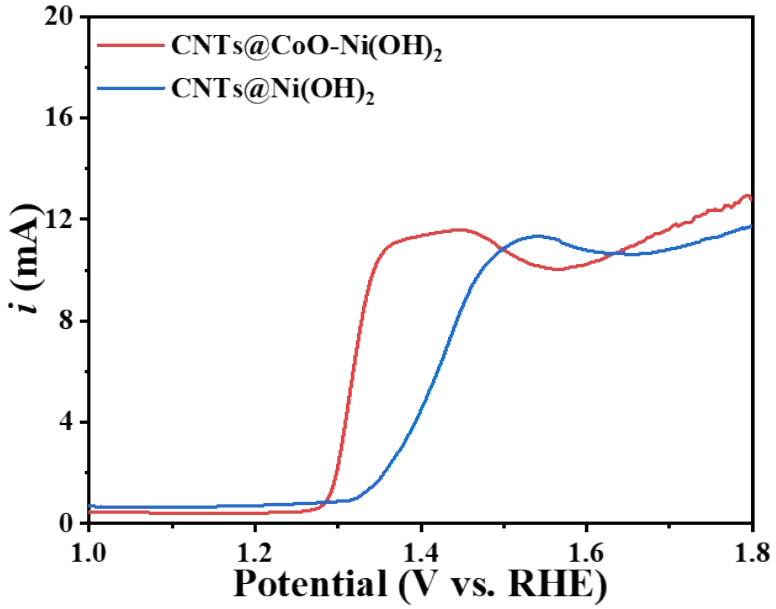

Figure S13 Differential pulse voltammetry (DPV) curves of the CNTs@CoO-$Ni(OH)_2$ and CNTs@$Ni(OH)_2$ composites.

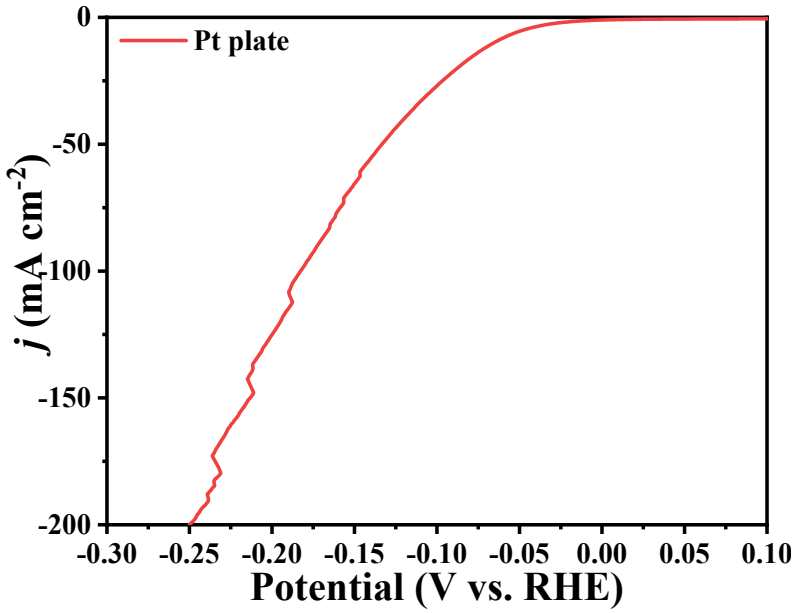

Figure S14 LSV curves of the Pt plate electrode in 1 M KOH+1 M MeOH.

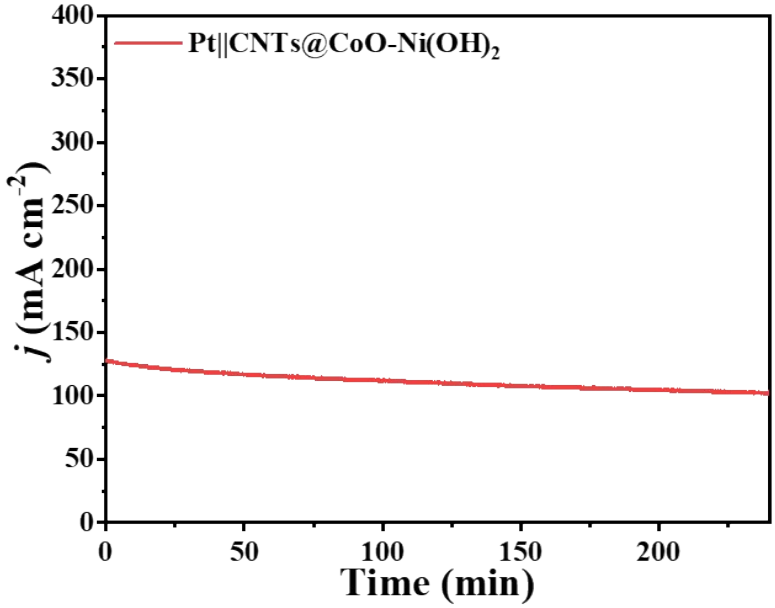

Figure S15 Chronoamperometry (i-t) curves of the Pt||CNTs@CoO-Ni(OH)$_2$ device in 1 M KOH +1 M CH_3OH.

Table S1 MOR performance comparison of reported electrocatalysts.

Electrocatalysts	Electrolyte	Current density at reported potential (mA cm^{-2})	Tafel slope (mV dec^{-1})	Product	Reference
CNTs@CoO-$Ni(OH)_2$	**1.0 M KOH+1.0 M MeOH**	**100 @ 1.36 V**	**43.9**	**Formate**	**This work**
CC@$NiCo_2S_4$	1.0 M KOH+1.0 M MeOH	100 @ 1.40 V	39.9	Formate	[1]
NiSe/$MoSe_2$/CC	1.0 M KOH+1.0 M MeOH	100 @ 1.38 V	14.0	Formate	[2]
NiO/NF	1.0 M KOH+1.0 M MeOH	100 @ 1.53 V	135.0	Formate	[3]
Ni_2P-CoP/NF	1.0 M KOH+0.5 M MeOH	100 @ 1.30 V	37.5	Formate	[4]
$Ni(OH)_2$/NF	1.0 M KOH+0.5 M MeOH	100 @ 1.36 V	17.6	Formate	[5]
Mo-Co_4N/CC	1.0 M KOH+3.0 M MeOH	10 @ 1.36 V	98	Formate	[6]
Fe_2O_3/NiO/NF	1.0 M KOH+1.0 M MeOH	500 @ 1.65 V	-	Formate	[7]

Table S2 the system resistance (R_s) and charge transfer resistance (R_{ct}) calculated from EIS data (MOR at 1.41 V vs. RHE)

Samples	$R_s(\Omega)$	$R_{ct}(\Omega)$
CNTs@CoO-Ni$(OH)_2$	2.05	1.27
CNTs@Ni$(OH)_2$	2.11	1.39
CoO-Ni$(OH)_2$/CC	2.46	1.30

Table S3 The values of surface coverage of (Γ^*) and proton diffusion coefficient (D)

Samples	Γ^* ($\times 10^{-6}$ mol cm^{-2})	D ($\times 10^{-6}$ cm^2 s^{-1})
CNTs@CoO-Ni(OH)$_2$	1.59	1.90
CNTs@Ni(OH)$_2$	1.19	1.51
CoO-Ni(OH)$_2$/CC	1.19	0.83

Reference:

1 F. Si, J. Liu, Y. Zhang, B. Zhao, Y. Liang, X. Wu, X. Kang, X. Yang, J. Zhang, X.-Z. Fu and J.-L. Luo, *Small*, 2023, **19**, 2205257.

2 X. Peng, S. Xie, X. Wang, C. Pi, Z. Liu, B. Gao, L. Hu, W. Xiao and P. K. Chu, *J. Mater. Chem. A*, 2022, **10**, 20761-20769.

3 M. I. Abdullah, A. Hameed, N. Zhang, M. H. Islam, M. Ma and B. G. Pollet, *ACS Appl. Mater. Interfaces*, 2021, **13**, 30603-30613.

4 D. Wu, J. Hao, W. Wang, Y. Yu, X.-Z. Fu and J.-L. Luo, *ChemSusChem*, 2021, **14**, 5450-5459.

5 J. Hao, J. Liu, D. Wu, M. Chen, Y. Liang, Q. Wang, L. Wang, X.-Z. Fu and J.-L. Luo, *Appl. Catal. B*, 2021, **281**, 119510.

6 T. Wang, X. Cao, H. Qin, X. Chen, J. Li and L. Jiao, *J. Mater. Chem. A*, 2021, **9**, 21094-21100.

7 Y. Hao, D. Yu, S. Zhu, C.-H. Kuo, Y.-M. Chang, L. Wang, H.-Y. Chen, M. Shao and S. Peng, *Energy Environ. Sci.*, 2023, **16**, 1100-1110.